JOURNAL OF SOLID STATE CHEMISTRY 105, 410–416 (1993)

Short Range and Long Range Magnetic Order in 1*T*-Li_2NiO_2

I. J. DAVIDSON*

Institute for Environmental Chemistry, National Research Council of Canada, Ottawa, Ontario, Canada K1A 0R6

J. E. GREEDAN

Institute for Materials Research and Department of Chemistry, McMaster University, Hamilton, Ontario, Canada L8S 4M1

U. VON SACKEN AND C. A. MICHAL

Moli Energy (1990) Ltd., 3958 Myrtle St., Burnaby, B.C., Canada V5C 4G2

AND W. R. MCKINNON

Institute for Microstructural Sciences, National Research Council of Canada, Ottawa, Ontario, Canada K1A 0R6

Received September 17, 1992; in revised form December 15, 1992; accepted December 16, 1992

The magnetic behavior of 1*T*-Li_2NiO_2 was examined by dc magnetization measurements and powder neutron diffraction. A magnetic structure was refined from low temperature powder neutron diffraction data. The low temperature magnetic structure is formed by antiferromagnetic coupling of ferromagnetically aligned nickel sheets, resulting in a doubling of the cell along the *c*-axis. The dc magnetization measurements show applied field and temperature dependence indicative of competition between long range antiferromagnetic ordering and short range ferromagnetic coupling, resulting in a metamagnetic transition.

I. Introduction

A novel phase of Li_2NiO_2 was recently prepared by an electrochemical, *chimie douce* approach (*1*). The crystal structure of this new phase was determined by Rietveld profile refinement of powder neutron diffraction data (*2*). This phase is isostructural with Li_2VSe_2 and Li_2MnO_2 (*3*), having a trigonal CdI_2 or 1 *T* type structure completely different from that of orthorhombic Li_2NiO_2 (*4*). The 1*T*-Li_2NiO_2 is composed of hexagonally close-packed layers of oxygen which alternate with layers of metal atoms in the sequence O–Ni–O–Li–O–Ni–O–Li.... The lithium atoms occupy tetrahedral interstices between the more broadly spaced oxygen layers, while the nickel atoms fill octahedral sites between the alternate, more closely spaced, oxygen layers. As the magnetic atoms are separated by three nonmagnetic sheets, this material could have substantial 2D character in its magnetic properties.

The hexagonal Li_2NiO_2 structure belongs to the space group $P\text{-}3m1$, with $a = 3.0954(9)$ Å and $c = 5.070(1)$ Å at 300 K. The nickel atom occupies the 1a position at (0, 0, 0), and the lithium and oxygen atoms the 2d sites at ($\frac{1}{3}$, $\frac{2}{3}$, 0.649) and ($\frac{1}{3}$, $\frac{2}{3}$, 0.2333), respectively. The nickel atoms occupy regular octahedral sites with an oxygen bond distance

* To whom correspondence should be addressed.

0022-4596/93 $5.00

of 2.143(1) Å. The lithium tetrahedra are elongated along the c-axis having one Li–O bond of 2.108(2) Å and three of 1.884(1) Å.

II. Experimental Details

1T-Li_2NiO_2 was prepared by reacting $LiNiO_2$ with a 1.5 M excess of Li^+ benzophenone$^-$ in tetrahydrofuran (THF) in an inert atmosphere glove box. After the mixture was stirred overnight, the powder was recovered by filtration. The black powder was rinsed with dry THF, and then dried under vacuum. This gave predominantly 1T-Li_2NiO_2 with a small percentage of unreacted $LiNiO_2$. 1T-Li_2NiO_2 prepared in this way is poorly crystalline. Sample crystallinity was improved by a careful annealing which avoided conversion to the orthorhombic form. This was accomplished by heating the sample at 225°C for 14 hr under a flow of dry helium. An X-ray powder diffraction pattern taken after the annealing procedure revealed a small amount of decomposition to NiO, which probably resulted from the presence of some moisture in the helium. Profile refinement of the powder neutron diffraction pattern collected at room temperautre indicated that NiO and $LiNiO_2$, combined, represent about 7% of the sample. Full details of the preparation method and the refinement of the chemical structure are given in Ref. (*2*).

Neutron powder diffraction data were collected at the McMaster Nuclear Reactor using 1.3913 Å neutrons obtained from a [200] copper monochromator and a spectrometer described in Ref. (*5*). The raw data were collected with a three-tube position-sensitive detector, and were corrected for the detector geometry according to the procedures of Ref. (*6*). Neutron diffraction patterns were gathered over a low angular range, to about 5° in 2θ, at various temperatures between 10 K and room temperature. The sample was held in an aluminum can which was sealed with an indium gasket in a helium atmosphere. The helium serves both as a heat exchange gas and to protect the air and moisture sensitive sample from chemical decomposition.

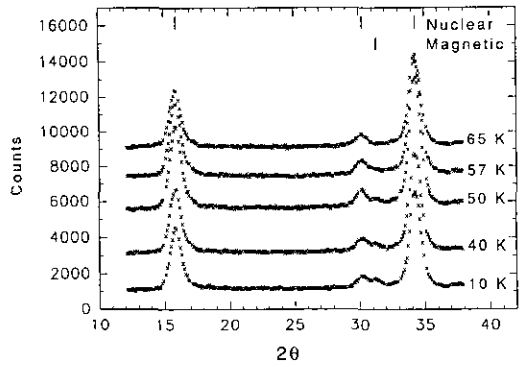

FIG. 1. *Powder neutron diffraction patterns of* Li_2NiO_2 over temperature range 65 to 10 K. The positions of nuclear and magnetic reflections are indicated at the top of the figure.

Dc magnetization was measured in a *Quantum Design* SQUID magnetometer. For the magnetization measurements, 16.01 mg of 1T-Li_2NiO_2 were contained in a crimp seal aluminum TGA capsule, which had been filled and sealed in a helium atmosphere glove box.

III. Results and Discussion

A. Magnetic Structure

Neutron powder diffraction patterns for the temperature range 65 to 10 K, shown in Fig. 1, indicate only one magnetic peak, at 31.2° in 2θ, which begins to form at about 57 K. The magnetic peak indexes as $(10\frac{1}{2})$ relative to the chemical cell, implying $c_{mag} = 2\,c_{chem}$ or a magnetic sublattice propagation vector $\mathbf{k} = (00\frac{1}{2})$.

A neutron powder diffraction pattern of Li_2NiO_2 was collected over a broader angular range at 10 K, and was analyzed with the Rietveld profile refinement program *Rietan* written by Izumi (*7*). This program is capable of modeling neutron scattering from magnetic structures with collinear spin arrangements. The magnetic moment, μ_j, of each magnetic site, and the angle between the spin direction and the unique axis of the

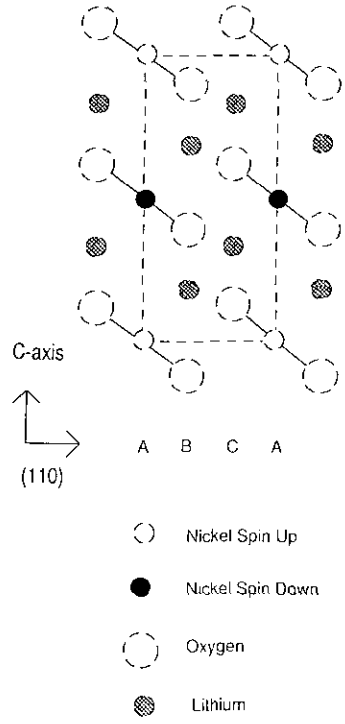

FIG. 2. $11\bar{2}0$ projection of magnetic cell with the c-axis vertical. The hexagonal unit cell is indicated by the dashed line.

lattice, Φ, can be refined using the equations given by Shirane (*8*). For these calculations, the magnetic moment of the nickel ion was taken as 2.0 μ_B, and the magnetic form factor determined for Ni^{2+} in NiO by Alperin (*9*) was used. The refinement was carried out in the chemical space group $P\text{-}3m1$ but with $c_{mag} = 2\,c_{chem}$, and the two nickel sites, 1a and 1b, were allowed different spin orientations. Figure 2 is the $11\bar{2}0$ projection of the doubled $1T$ cell with the c-axis vertical. The dashed line indicates the hexagonal cell. The nickel atoms separated by two layers of lithium and oxygen atoms exhibit AAA stacking in the hexagonal close packed structure. Within the planes perpendicular to the c-axis, neighboring nickel atoms are linked through bonds to oxygen atoms at a bond angle of 92.5°. As the Goodenough–Kanamori rules predict ferromagnetic interactions for a 90° d^8–d^8 system, ferromagnetic order within the planes perpendicular to the c-axis can be anticipated (*10*). The absence of magnetic superlattice reflections assignable to expansion of the a or b axes supports this view, as do the bulk magnetic properties reported in the following section.

Thus, two structures, based on antiferromagnetically coupled ferromagnetic sheets, one with spins normal to c and the other with the spins parallel to c, were refined. The results are shown in Figs. 3a and 3b. The peak at 40° is due to the aluminum container and the shoulder at 39° results from residual NiO and $LiNiO_2$ from the synthesis of the material (*2*). Neither $LiNiO_2$ nor NiO contributes to the peak at 31.5° in 2θ. For $LiNiO_2$ no magnetic Bragg scattering has been observed at any temperature or angle (*11*). The low temperature neutron diffraction pattern of NiO was investigated by Roth (*12*). As shown by Fig. 3b, the model with the magnetic moments parallel to the c axis is a good fit to the observed intensities. The details of this Rietveld refinement are tabulated in Table I. The atomic positions were fixed at the sites determined previously from the room temperature powder neutron diffraction data (*2*). The three background parameters, the scale, the zero-point shift, and two lattice parameters were allowed to refine. The structure remained unchanged on cooling to 10 K. However, both the a and c axes shrank slightly, thereby reducing the cell volume by 1.2%. Releasing the magnetic moment for refinement gave a value of (1.40 ± 0.49) μ_B with no improvement in the profile fit.

B. Magnetization Studies

An apparent susceptibility can be calculated by dividing the dc magnetization by the applied field, M/H. The plot of M/H against temperature, Fig. 4, is indicative of an antiferromagnet with a T_N of 64 K, but as the inset figure shows, the magnetization does not fit Curie–Weiss behavior. In the plot of magnetic moment versus applied field to 2.0 T, Fig. 5, the moment is linearly

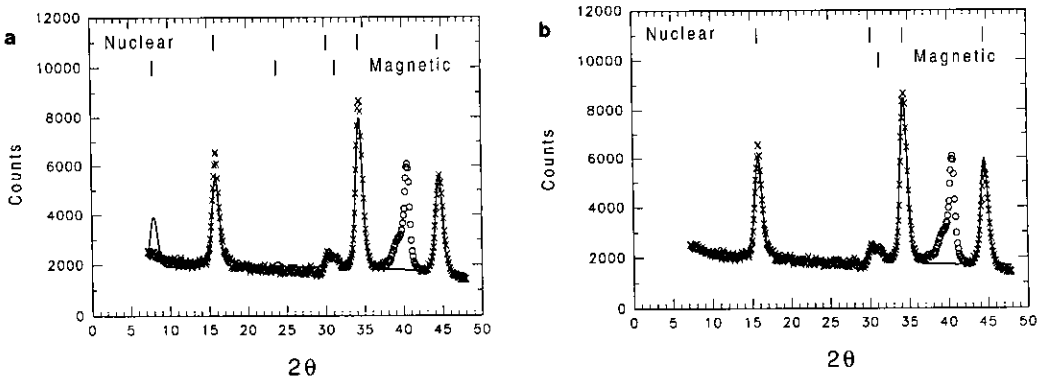

FIG. 3. Powder neutron diffraction pattern for Li_2NiO_2 at 10 K is represented with symbols while the lines represent Rietveld refinement fits with (a) spin perpendicular to c-axis and (b) spin parallel to c-axis. The positions of nuclear and magnetic reflections are indicated at the top of the figures.

dependent on the applied field for $T = 10$ K and 30 K. Hence the magnetic behavior is consistent with long range antiferromagnetic ordering (LRAFO) for $T < T_N$. However, when the applied field is raised to 5.0 T the observed moments, shown in Fig. 6, are much larger than expected based on a linear extrapolation of the lower field data. In fact, at 5.0 T, the actual moments are quite substantial, 1.27 μ_B/Ni^{+2} at 10 K. The change in slope of the magnetic moment between 2.0 and 5.0 T and the large observed moments at high field indicate a metamagnetic transition. Replotting the moment versus field data as moment versus temperature (Fig. 7) shows that the maximum disappears for the $B = 5.0$ T case. The small quantities of NiO and $LiNiO_2$ present in our sample are not expected to interfere with the interpretation of the magnetization studies. NiO

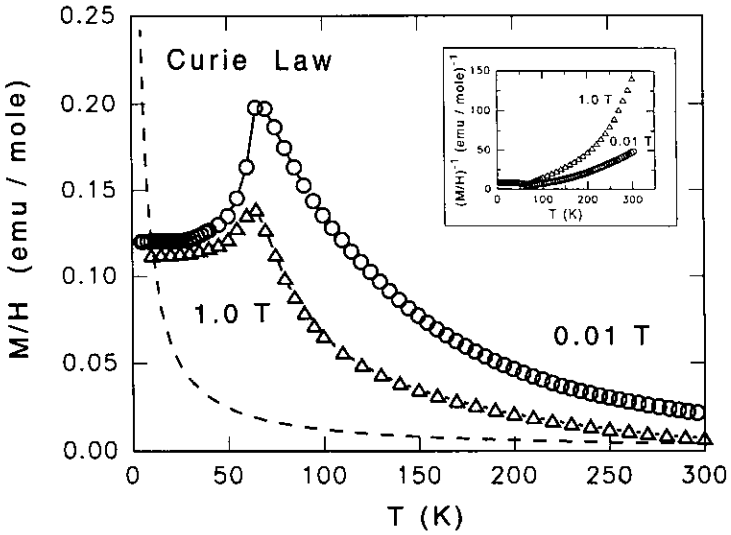

FIG. 4. Magnetization divided by applied field is plotted against temperature for applied fields of (a) 0.01 T (circles) and (b) 1.0 T (triangles). Dashed line indicates a Curie law fit to values for Ni^{2+} ($S = 1$ and $g = 2.2$). The inset figure shows the inverse of M/H versus temperature.

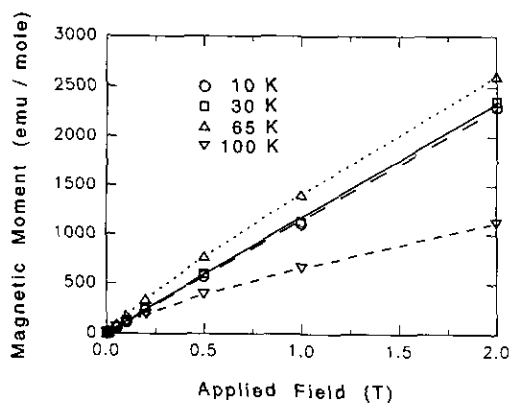

FIG. 5. Magnetic moment as a function of temperature versus applied field to 2.0 T.

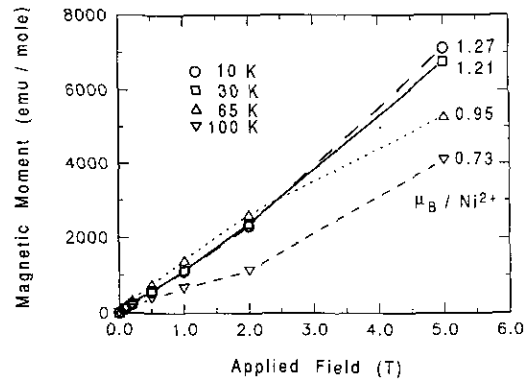

FIG. 6. Magnetic moment as a function of temperature versus applied field to 5.0 T.

is an antiferromagnet with a T_N = 523 K. (*13*) In a recent study of $LiNiO_2$ (*14*), the observed values of the molar susceptibility were lower by a factor of 5 or more than those of Li_2NiO_2 at the same temperature. Thus the contribution of $LiNiO_2$ to the measured magnetization of our sample would be at the 1–2% level.

The M/H versus T data for $T > T_N$ show that the measured M/H values are always higher than the values predicted by the Curie Law and that M/H is field dependent.

TABLE I

RIETVELD REFINEMENT OF 10 K NEUTRON DIFFRACTION DATA FOR Li_2NiO_2 WITH SPINS ALIGNED PARALLEL TO THE c-AXIS

Atom	x	y	z	Moment (μ_B)	Occupancy
Ni (1a)	0.0	0.0	0.0	2.0	1.0
Ni (1b)	0.0	0.0	0.5	−2.0	1.0
Li (2d)	$\frac{1}{3}$	$\frac{2}{3}$	0.3245		1.0
Li (2d)	$\frac{1}{3}$	$\frac{2}{3}$	0.8245		1.0
O (2d)	$\frac{1}{3}$	$\frac{2}{3}$	0.1167		1.0
O (2d)	$\frac{1}{3}$	$\frac{2}{3}$	0.6167		1.0

Note. Space group $P\text{-}3m1$ (D_{3d}^3); lattice parameters a = 3.080(2) Å and c = 10.118(8) Å; overall temperature factor B = 0.05 Å^2; halfwidth parameters U = 1.80, V = −1.20, W = 1.31; scattering lengths Ni 1.030, Li −0.203, O 0.5805; weighted profile R = 6.01, profile R = 4.79, Bragg R = 3.56, expected R = 2.00.

This can only be due to ferromagnetically coupled domains or clusters of subcritical size within the layers. The domain size distribution and moment distribution are temperature and field dependent. The moment versus field curves for T = 65 K and 100 K (Fig. 5) show curvature consistent with ferromagnetic correlations. At 65 K, the moment versus field data shows a smooth increase up to 5.0 T where a large moment of about 1.0 μ_B/Ni^{+2} is found. The 100 K data show a slope change between the ranges below 2.0 T and above 2.0 T, indicating a more complex short range ordered microstructure. Even at T = 300 K, the apparent susceptibility, M/H, is different for applied fields of 0.01 and 1.0 T. The nonlinear field dependence at T = 300 K indicates that the short range ferromagnetic order persists above room temperature.

IV. Summary and Conclusions

The magnetic behavior of 1T-Li_2NiO_2 is best described by division into two regimes, long range antiferromagnetic order for $T <$ about 60 K and short range ferromagnetic order for $T >$ 60 K. The long range antiferromagnetic state is well characterized by the neutron powder diffraction data. The magnetic structure consists of ferromagnetic sheets coupled antiferromagnetically with a moment direction parallel to the c-axis and a

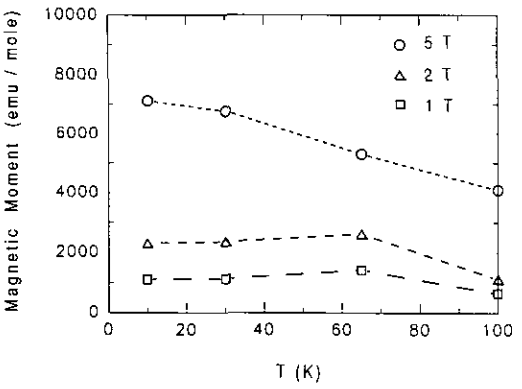

FIG. 7. Magnetic moment data replotted as moment versus temperature for various applied fields.

moment value close to 2.0 μ_B. The ordering onset temperature from the neutron data, T_N = 57 to 60 K, is a bit lower than the temperature of the maximum value of M/H, but this is not unusual.

The dc magnetization measurements on 1T-Li_2NiO_2 at applied fields up to 2.0 T indicate antiferromagnetic ordering with a T_N of 64 K. Somewhere between 2.0 and 5.0 T a metamagnetic transition occurs such that by 5.0 T the magnetic behavior is dominated by short range ferromagnetic coupling. Even in the low field range, up to 2.0 T there is clear evidence of ferromagnetic correlations in the magnetic data collected at or above 65 K.

These results can be compared to those for the anhydrous dichlorides of the first row transition metals, e.g., $FeCl_2$, $CoCl_2$, and especially $NiCl_2$. These materials have the layer-type $CdCl_2$ structure, which is similar to that of 1T-Li_2NiO_2. The three dihalides mentioned have strong ferromagnetic intraplanar exchange and weak interplanar antiferromagnetic exchange (*15*). At zero applied field the ground state magnetic structures consist of antiferromagnetically coupled ferromagnetic layers as found for 1T-Li_2NiO_2 (*16*). All show metamagnetic transitions at low temperatures. For example, the critical field for $FeCl_2$ at 4.2 K is 1.1 T (*17*). Of the group $NiCl_2$ has the highest antiferromagnetic transition temperature of 52 K, remarkably close to the 65 K reported here for 1T-Li_2NiO_2. Presumably, the strong intraplanar ferromagnetic correlations result from the 90° M–Cl–M linkages. Evidence for the presence of short range ordered ferromagnetic clusters above the long range ordering temperature has been found in $FeCl_2$ from small angle neutron scattering (SANS) (*16*). Similar short range order is reported here for 1T-Li_2NiO_2. SANS measurements on this material will be undertaken in the near future. The main difference between $NiCl_2$ and 1T-Li_2NiO_2 is the preferred direction for the Ni^{2+} moments, which is normal to the c-axis in the former and parallel to the c-axis in the latter.

Acknowledgment

J.E.G. acknowledges financial assistance from the Natural Science and Engineering Research Council of Canada.

References

1. J. R. DAHN, U. VON SACKEN, AND C. A. MICHAL, *Solid State Ionics* **44**, 87 (1990).
2. I. DAVIDSON, J. E. GREEDAN, U. VON SACKEN, C. A. MICHAL, AND J. R. DAHN, *Solid State Ionics* **46**, 243 (1991).
3. W. I. F. DAVID, J. B. GOODENOUGH, M. M. THACKERAY, AND M. G. S. R. THOMAS, *Rev. Chim. Miner.* **20**, 636 (1983).
4. H. RIECK AND R. HOPPE, *Z. Anorg. Allg. Chem.* **392**, 193 (1972).
5. J. E. GREEDAN AND A. H. O'REILLY, *Phys. Rev. B* **35**, 8770 (1987).
6. C. W. TOMPSON, D. F. R. MILDNER, M. MEHREG-

ANG, J. SUDOL, R. BERLINER, AND W. B. YELON, *J. Appl. Crystallogr.* **17,** 385 (1984).
7. F. IZUMI, "Rietan–Rietveld Analysis System," National Institute for Research in Inorganic Materials, Ibaraki.
8. G. SHIRANE, *Acta Crystallogr.* **12,** 282 (1959).
9. H. A. ALPERIN, *J. Phys. Soc. Jpn.* **17** (Suppl. B-III), 12 (1962).
10. J. B. GOODENOUGH, "Magnetism and the Chemical Bond," p. 180, Interscience, New York (1963); J. A. BERTRAND, A. P. GINSBERG, R. I. KAPLAN, C. E. KIRKWOOD, R. L. MARTIN, AND R. C. SHERWOOD, *Inorg. Chem.* **10,** 240 (1971).
11. K. HIRAKAWA AND H. KADOWAKI, *Physica B* **136,** 335 (1986).
12. W. L. ROTH, *Phys. Rev.* **110,** 1333 (1958).
13. H. KONDOH, *J. Phys. Soc. Jpn.* **15,** 1970 (1960).
14. J. N . REIMERS, J. R. DAHN, J. E. GREEDAN, C. V. STAGER, G. LIU, I. DAVIDSON, AND U. VON SACKEN, *J. Solid State Chem.* **102,** 542 (1993).
15. C. STARR, F. BITTER, AND A. R. KAUFMANN, *Phys. Rev.* **58,** 977 (1940); H. BIZETTE, C. TERRIER, AND B. TSAI, *C. R. Hebd. Seances Acad. Sci.* **243,** 895, 1295 (1956); R. J. BIRGENEAU, W. B. YELON, E. COHEN, AND J. MAKOVSKY, *Phys. Rev. B* **5** 2607 (1972); and earlier references cited therein.
16. M. K. WILKINSON, J. W. CABLE, E. O. WOLLAN AND W. C. KOEHLER, *Phys. Rev.* **113,** 497 (1959); D. BILLEREY, C. TERRIER, R. MAINARD, AND P. MERIEL, *C. R. Seances Acad. Sci. Ser. B* **284,** 495 (1977).
17. I. S. JACOBS AND P. E. LAWRENCE, *Phys. Rev.* **164,** 866 (1967).